Using Finite-Element Method for Analyzing the Effect of Coriolis Acceleration on the Ring- Spinning Balloon

Nematallah Mardani Mehrabad[i]; Majid Safar Johari[ii]; Mohammad Mohammadi Aghdam[iii]

ABSTRACT

This study is aimed at deriving a dynamic theory of twist insertion in the ring-spinning balloon and diagnosing the effects of Coriolis acceleration on the yarn tension and configuration. To do so, the relationship between twist insertion and tension of the yarn was explained. The yarn tension at the pigtail in the ring spinning machine was measured by a novel set up; in which, traveler revolution (r.p.m.) was also sensed. The results were used in a simulation program as the boundary values. For simulation, a computer model in finite element method (FEM) was introduced, which can predict the effect of the existing forces on the stress distribution. It was observed that the equations, governing the yarn path, and the movement equation of twist in the yarn were completely dependent on each other. The Coriolis acceleration had a little effect on the balloon configuration, although it made tension in the yarn. Nevertheless, to obtain better and more accurate results, Coriolis acceleration might be taken into consideration.

KEYWORDS

yarn balloon; Coriolis acceleration; finite element method; twist insertion.

1. INTRODUCTION

Among different existing spinning methods, the ring spinning is still the most suitable method of producing fine and high-quality yarns. In the ring spinning, power consumption and ends-down are closely related to spinning tension and spindle speed [1]. Moreover, spinning tension affects the structure and properties of spun yarns [1]. So, the researchers have tried to predict the yarn tension and ring spinning balloon's profiles (i.e., the looping portion of the yarn between the pigtail guide and the traveler). Almost fifty years after ring-spinning method invention by John Thorp in 1828, the dynamic balloon theory was studied by Lüdicke. The study of the mathematical models has been started since 1950s, followed by the different aspects of yarn balloon such as configuration and tension. Grishin [13] attempted to report the dynamic theory of the yarn balloon. A great review on the state-of-the art up to late 1980s can be found in the paper by Batra *et al.* [2]. Zeng [1] also carried out a complete review as well until the late 1990s. Clark *et al.* [3], Fraser *et al.* [4] -[7] and Tang *et al.*[15] investigated the dynamic theory, the effect of non-uniformity and slob on the stability and simulation of the ring spinning balloon. However, none of the previous researchers paid special attention to the effect of Coriolis acceleration and twist on the stress distribution in the spinning balloon.

Therefore, in this research, Coriolis acceleration is considered as it makes tension in the yarn and is dependent to the twist.

2. EQUATIONS GOVERNING THE YARN PATH AND TWIST INSERTION

In the ring twisting process, the yarn is passed through different regions from delivery rolls to bobbin. In each zone, the yarn takes a different shape. It can result a motion as shown in Figure 1.

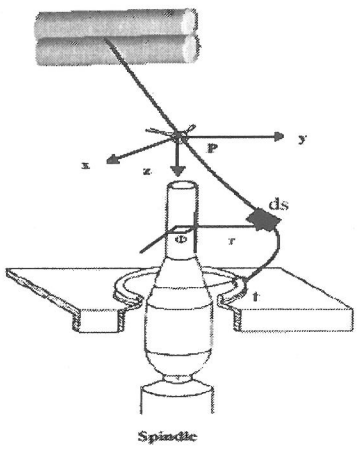

Figure 1: Ring spinning.

The region between pigtail (p) and traveler (t) is called balloon, produced by rotating the traveler around the bobbin axis that is assumed to be quasi-stationary. Since the yarn is considered to be uniform in mass linear density, the problem does not depend on time.

i N. Mardani Mehrabad is with Department of Textile Engineering, Amirkabir University of Technology, Tehran, IRAN (e-mail: mardan1352@yahoo.com).

ii M. Safar Johari is with Department of Textile Engineering, Amirkabir University of Technology, Tehran, IRAN (e-mail: mjohari@aut.ac.ir).

iii M. M. Aghdam is with Department of Mechanical Engineering, Amirkabir University of Technology, Tehran, IRAN (e-mail: aghdam@aut.ac.ir).

Meanwhile, in related analyses, where researchers consider a small yarn segment (ds) along with a yarn tension (T_s) and by an imaginary position, have determined the motion equation of the segment as (1).

$$F+\frac{d(Tt)}{ds}=0 \quad (1)$$

where $t(\frac{dr}{ds}, r\frac{d\phi}{ds}, \frac{dz}{ds})$ is a vector tangent unit to the yarn, directed towards the increasing s co-ordinate. Force F is the sum of air drag and weight, plus centrifugal and Coriolis force and inertial force of the linear index motion.

Before Batra *et al.* [2] none of the researchers predicted balloon configuration and spinning tension simultaneously. But they overcame these difficulties and the extracted formula is the same as (2) - (6).

$$F_o=-\frac{1}{2}C_n\rho D|V_n|V_n \quad (2)$$

$$\frac{d}{ds}(T_s\frac{dr}{ds})-T_s r(\frac{d\phi}{ds})^2+\frac{\mu_0}{f(T)}\omega^2 r+2\frac{\mu_0}{f(T)}w\omega r\frac{d\phi}{ds}+F_{or}=0 \quad (3)$$

$$\frac{1}{r}\frac{d}{ds}(T_s r^2\frac{d\phi}{ds})-2\frac{\mu_0}{f(T)}w\omega\frac{dr}{ds}+F_{o\phi}=0 \quad (4)$$

$$\frac{d}{ds}(T_s\frac{dz}{ds})+\frac{\mu_0}{f(T)}g+F_{oz}=0 \quad (5)$$

$$T_s=T-\frac{\mu_0}{f(T)}w^2,\frac{ds}{dL}=f(T),(\frac{dr}{ds})^2+r^2(\frac{d\phi}{ds})^2+(\frac{dz}{ds})^2=1 \quad (6)$$

The nonlinear differential equation of balloon dynamics involves the second order, ordinary differential equations (ODEs). In practice, it is not possible to solve it analytically; so it must necessarily be solved by the numerical methods such as finite element method.

Since the amount of the Coriolis acceleration is negligible compared to other accelerations in the balloon area, it has usually been ignored at balloon configuration prediction. According to [4], Coriolis acceleration has no significant effect on balloon dynamics. Fraser and Stump [7] tried to consider the twist in balloon but did not pay attention to the effect of Coriolis acceleration in the real situation. They concluded that "the equations governing the yarn path and the equations governing the movement of twist along the yarn path are independent of each other."

Meanwhile, the results of this research show that those two equations (yarn path & movement of twist) are dependent on each other and in the case of twist, Coriolis acceleration has to be considered.

A closer look at the gyroscopic movement of the yarn in Figure 2 reveals that the relationship between the twist insertion speed ($\omega 1$) and the traveler revolution ($\omega 2$) in case the inertial moment is I can be as (7).

$$M_o=I(\omega 1)(\omega 2) \quad (7)$$

M_o is the moment vector, goes around the z axis, proving the dependency of twist and traveler revolution.

Furthermore, according to [7] if T_w is the yarn twist (turns per unit length) then its relation to angular movement $(d\varphi)$ is :

$$T_w=\frac{1}{2\pi}\frac{d\varphi}{ds} \quad (8)$$

Then, if φ component of air drag in [2] is negligible, it can be mentioned that:

$$\frac{dT_\varphi}{dr}=m(2\omega V_p) \quad (9)$$

$$\frac{dT_\varphi}{dr}=T\frac{d\varphi}{ds} \quad (10)$$

By considering (8)-(10), it can be concluded that:

$$T_w=\frac{m(2\omega V_p)}{2\pi T} \quad (11)$$

Hence, (11) shows the relationship between twist of the yarn (T_w), Coriolis acceleration (ωV_p) and balloon tension (T). It shows that twist and Coriolis acceleration are directly dependent on each other.

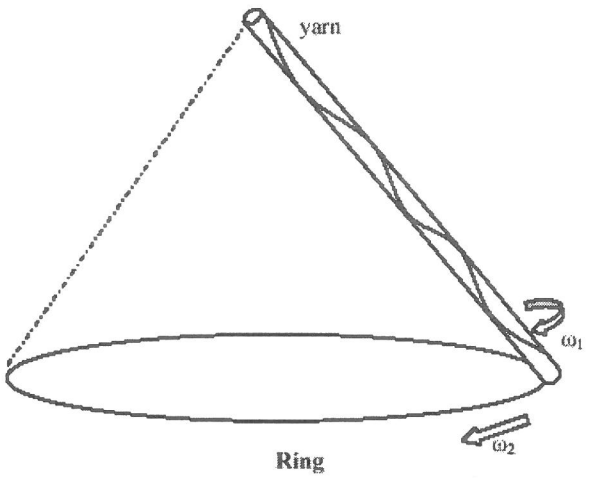

Figure 2: Yarn twist and traveler revolution.

3. FINITE-ELEMENT METHOD AND YARN BALLOON

Finite-element method is one of the most suitable ways to study the structures numerically. The history of its usages from military to textile industry can be found elsewhere [8]. Its advantages can be compared to other

numerical techniques, like easy work with non-homogeneous and non-linear media. The application of the finite element analysis in textile problems was first initiated by Lloyd *et al.* [14] and introduced to yarn structure by Van Luijk *et al.* [9] later. Van Luijk *et al.* [10-11] applied this method to both continuous filament and staple yarns. There have also been several activities in other textile-related fields, like the paper by Zako *et al.* [12]. Hence, FEM is utilized because of its great ability to study the stress-strain distribution in structures.

A. Related Element

In this research SOLID95 elements are used. These elements are usually used to model 3D structures. As they have compatible displacement shapes are well suited to model the yarn. The element is defined by 20 nodes having three degrees of freedom per node (Figure 3).

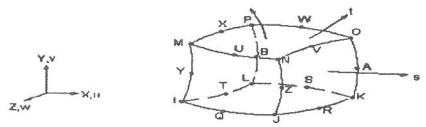

Figure 3: 20 Nodes SOLID95 element.

B. Force Insertion

The balloon is divided into 8 nearly equal dimensionally elements. All the related forces as follow are put in each node as inputs (Figure 4).

The air drag is assumed to act in the direction, opposite to the yarn velocity component, normal to the thread line, proportional to the square of the magnitude of this normal velocity component. The air drag coefficient is assumed to be constant along with the whole length of the ballooning yarn.

Coriolis force which has the least effect comparison to the other forces acts perpendicularly to the plane in which the element lies. During spinning, its direction is opposite to the direction of the element circular movement, when the latter is above the maximum radius of the balloon, and in the same direction, when the element is below this maximum radius. Centrifugal force which is the most important and effective force acts along the radius r . The yarn tension at the pigtail and traveler revolution are measured experimentally. The average of the pigtail tension are used in simulation by FEM as the boundary axial values.

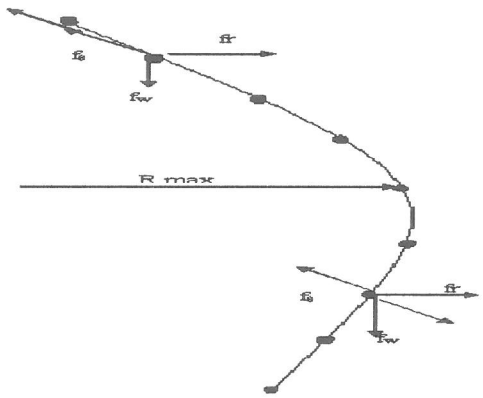

Figure 4: Force insertion in each node of balloon elements.

C. Yarn Physical Characteristics

In this research the effect of twist and its relationship with the Coriolis acceleration is considered. So the following example is mentioned to show the effect of Coriolis acceleration and twist in the balloon configuration. Experimentally the twist Coefficient of Variation is 7.8.

Yarn modulus, Pa	7×10^{10}
Poisson's ratio	0.3
Yarn fineness, Nm	50
Twist per meter	600
r.p.m. (Spindle speed)	18000
Balloon's height, cm	25

4. EXPERIMENTAL TENSION MEASUREMENT OF YARN BALLOON

The fibers string at the pigtail are so fine and unstable. It makes impossible to use the existing tension meters in ring spinning machine. Present experiences show that for fine counts, using tension meters causes the yarn to break. Tension meters can be used just for coarse yarns and the method is regarded as a destructive measurement. However, this method--since there is no extra contact with other instruments-- can be considered as nondestructive.

The yarn tension at the pigtail along with traveler revolution is measured simultaneously (Figure 5). The spinning machine is an SKF lab spinner. For measurement, four strain gauges (350Ω, Grid Length Measurement: 6mm) are assembled to the plate behind the pigtail , connected with a Wheatstone bridge.

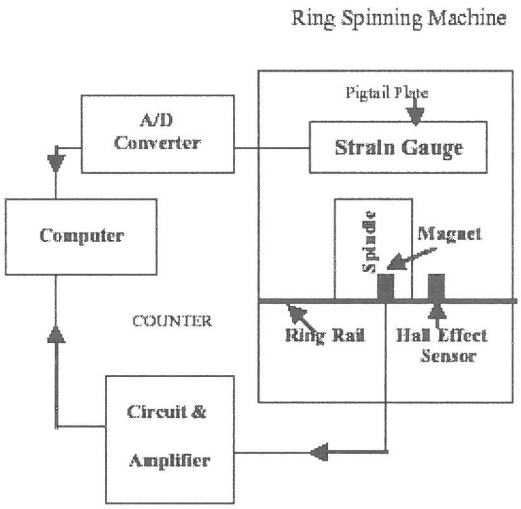

Figure 5: Experimental setup.

Authors' experiences show that to measure yarn tension horizontal index, all the strain gauges should be assembled at the top side of the plate (Figure 6). But as vertical indices are the subject of measurement, just a couple of them should be assembled at the bottom side of the plate (Figure 7).

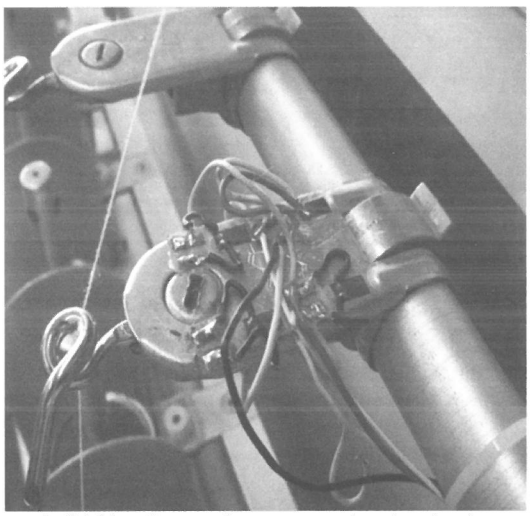

Figure 6: Sticking four strain gauges to the plate by the special glue.

As the yarn passes through the pigtail, vertical index of the yarn tension (F_z) which pigtail friction does not affect on, makes the plate bend. Thus, it increases the strain gauge length, changing their resistance and bridge voltage.

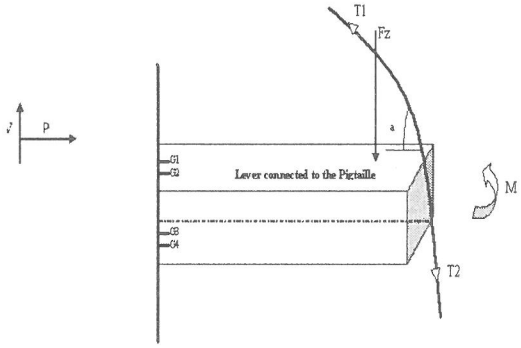

Figure 7: The configuration of experimental set up.

According to Figure 7:

$$T1 \sin a = F_z = V \quad (12)$$

$$T1 \cos a = P \quad (13)$$

$$T2 = T1\, e^{\mu a} \quad (14)$$

The changes in the voltage passing through an A/D converter, which amplifies and digits the output signals to transfer into the computer.

The spindle speed is sensed by a 3113 hall-effect sensor and a magnet attached to a spindle. Instead of each spindle rotation, the magnet once passes through the sensor and each time produces a signal. The number of signals per minute indicates the velocity of the spindle, which is added up to the related circuit. The results are transferred to the computer and drawn to the monitor by a special program, written to receive the results. At the same time, yarn tension at the pigtail and traveler revolution speed is drawn by graphs (Figure 8). The top graph in Figure 8 is the tension at the pigtail and the lower one is traveler speed. In Figure 8 horizontal axes are the rate of samples per unit time. It is about 10000 samples per minute. As it is possible to save the results, the screen has changed in a while completely.

Vertical axis in Figure 8 (top) shows the tension of yarn at the pigtail. Its results can be utilized in simulation. In practice as the ring rail traverses up/down, the tension will differ a bit. The tension of the yarn at the pigtail when the ring rail goes up is more than coming down. It can be because of wrapping the yarn around the smaller radius of the bobbin and smaller balloon height. Vertical axis of Figure 8 (down) represents the spindle revolution (r. p. m.) in each sample measurement. It is related to just one turn of ring rail (one up/down ward movement of ring rail). The experimental boundary axial values explained in 3.B are taken by Figure 8 (Top).

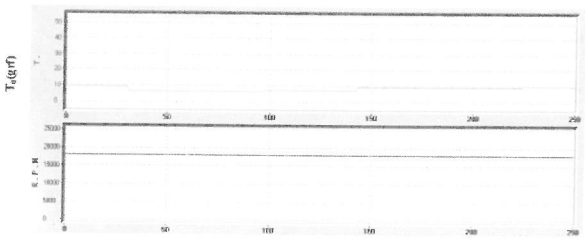

Figure 8: Tension changes at the pigtail and spindle revolution.

D. Calibration

A yarn thread is passed through the production path in the ring- spinning machine in order to simulate the yarn path during production. Then different weights are hung to the end of the yarn. The outputs are read on the monitor in stead of each weight. Considering the relationship between weights (in fact the tension exerted on the yarn) and the outputs, it is found that the relationship is linear. So using linear regression and applying the related indices, the output numbers will represent the real value of tensions with an error of less than five percent.

5. FEM MODELING RESULTS

All existing forces are put in the yarn as explained in section (3.B). The experimental results are also used as boundary axial values. The results of FEM modeling are shown in Figures 9 and 10. Figure 9 shows the balloon configuration. Experimentally, the balloon configurations have been taken by a G10 Canon Camera. In comparison with other researcher's results [1], the outputs can predict the balloon configuration with less approximation, since the role of the twist is also considered. Figure 10 shows the stress distribution of the balloon as well. The results are similar to the related equation mentioned in [2]. It shows that the maximum tension located near the pigtail.

If the predicted picture in Figure 9 is compared to the previous plots [1], the effect of Coriolis acceleration and twist is the same as Figure 11, making the results almost closer to the real situation.

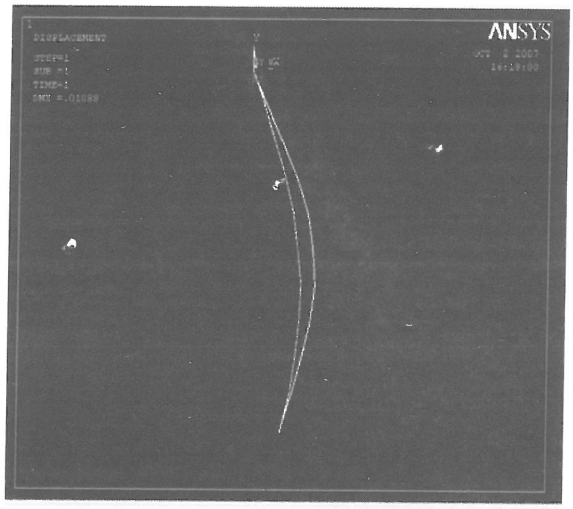

Figure 9: Prediction of balloon configuration.

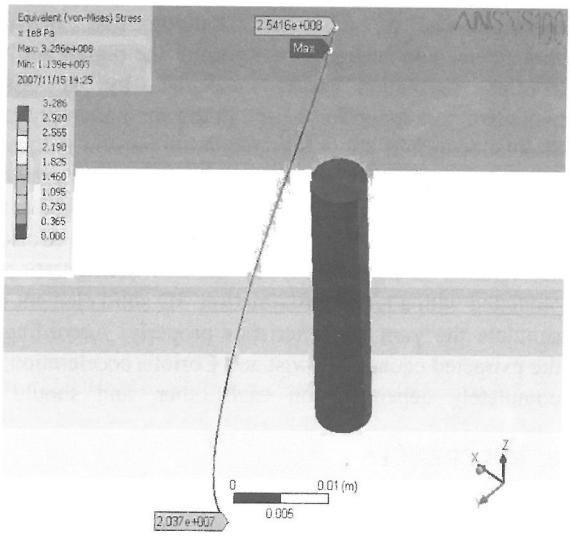

Figure 10: FEM modeling result of yarn balloon.

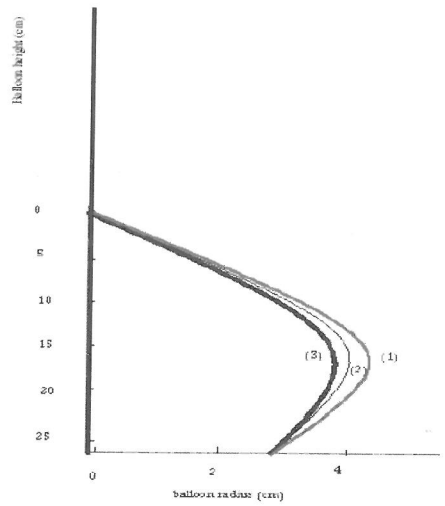

Figure 11: Balloon profile.

Figure 11-1: Experimental.
Figure 11-2: Predicted balloon profile with Coriolis acceleration.
Figure11-3: Predicted balloon profile without Coriolis acceleration.

6. CONCLUSIONS

Previous researchers omitted the effect of Coriolis acceleration. They believed that the amount of production velocity (V_p) is negligible compared to the revolution velocity ($r\omega$). As they tried to draw the balloon configuration, it did not have a significant effect. If twist insertion in the yarn is considered, Coriolis acceleration should not be omitted. In this research the effects of Coriolis acceleration and twist insertion in the balloon configuration and their relationship are studied, having been simulated numerically by entering the exact characteristics of the yarn, balloon and machine parameters. The tension of the yarn at the pigtail and the traveler revolution was measured by a novel nondestructive set up to be used in the simulation process. Simulation results show that maximum tension is located near the pigtail. That almost verifies the previous observations, which the ends-down can be occurred at the top much more. As the twist force and Coriolis acceleration is considered, the balloon configuration is predicted with a less approximation. 3D solid element can simulate the yarn characteristics properly. According to the extracted equations, twist and Coriolis acceleration are completely dependent on each other, and should be considered together in the calculations.

7. NOMENCLATURE

$F_{or}, F_{o\varphi}, F_{oz}$	Component of air drag force, N
T_r, T_φ, T_z	Component of yarn tension, N
ρ	Air drag density
D	Effective diameter of the yarn, mm
V_p	Production velocity of yarn, m/s
V_n	Vector of normal velocity component, m/s
C_n	The air drag coefficient (function of Reynolds number)
S	The length along the yarn, m
γ	Coefficient of friction
γ_0	Yarn mass per unit length, gr/m
m	Yarn mass, gr
w	Linear velocity of the yarn, m/s
L	Un loading length of the yarn, m
Nm	Metric yarn count (fineness)
μ	Yarn coefficient of friction
f_r, f_w, f_θ	Force component, N

8. REFERENCES

Dissertation:

[1] Q. Zeng, "Theoretical analysis of ring spinning" , Ph.D. dissertation, Faculty of North Carolina State University, 1995.

Periodicals:

[2] S. K. Batra, T. K. Ghosh, and M. I. Zeidman, "An integrated approach to dynamic analysis of the ring spinning process. Part I : Without air drag and Coriolis acceleration", Textile Res.J., vol. 59, pp. 309-317, 1989.

[3] J. D. Clark, W. B. Fraser, R. Sharma, and C. D. Rahn, "The dynamic response of a ballooning yarn: Theory and experiment", Proc. R.Soc.Lond. A454, pp. 2767-2789, 1998.

[4] W. B. Fraser, "On the theory of ring spinning", Phil. Trans. R. Lond, A342, pp. 439-468, 1993.

[5] W. B. Fraser, L. Farnell, and D. M. Stump, "Effect of yarn non-uniformity on the stability of the ring-spinning balloon", Proc. R. Soc. Lond. pp. 449-621, 1995.

[6] W. B. Fraser, L. Famell, and D. M. Stump, " The effect of a slob on the stability of the ring-spinning balloon", J. Text. Inst. 86, No4, pp. 610-634, 1995.

[7] W. B. Fraser, and D. M. Stump, "Yarn twist in the ring-spinning balloon", Proc. R. Soc. Lond. A, 457, pp. 707-723, 1998.

[8] A. J. Carr, P. J. Moss, and G. A. Carnaby, "The Tangent compliance matrix of wool industry", The Textile Inst. N. I. Section, P.P.193-203, 1988.

Dissertation:

[9] C.J. Van Luijk, "Structural analysis of wool yarns", Ph.D. dissertation, Dept. of civil Eng, Univ. of Cantrbury, 1981.

Periodicals:

[10] C. J. Van Luijk, A. J. Carr, and G. A. Carnaby, "Finite-Element analysis of yarns part I, II", J. Textile Inst. , vol. 75, pp. 342-362, 1984.

[11] C. J. Van Luijk, A. J. Carr, and G. A. Carnaby, "The Mathematics of staple-fiber yarns part I: Modeling Assumptions", J. Textile Inst. , vol. 76, pp. 11-18, 1985.

[12] M. Zako, Y. Uetsuji, and T. Kurashiki, "Finite element analysis of damaged woven fabric composite materials", Composites science and technology, vol. 63, pp. 507-516, 2003.

Books:

[13] P. F. Grishin, *Balloon control*, F.T.I Oldham. Platt Bros. Ltd., 1956.

[14] D.W. Van Lloyd, J.W.S. Hearle, J.J. Thwaites, , J. Amirbayat, Eds. sijthoff, and Noordhoff, "The Analysis of complex fabric deformations" in *Mechanics of Flexible Fiber Assemblies*, Proc. R.Soc.Lond., 1980, PP. 311-342.

Periodical:

[15] Z. Tang, X. Wang, W. B. Fraser, L. Wang, "Simulation and experimental validation of a ring spinning process", Simulation Modeling Practice and Theory, vol. 14, No. 7, pp. 809-816, 2006.